The International Journal of Advanced Manufacturing Technology (2020) 108:1125–1138
https://doi.org/10.1007/s00170-019-04877-7

ORIGINAL ARTICLE

Direct observation of discharging phenomena in vibration-assisted micro-electrical discharge machining

Tatsuya Shitara[1] · Kenjiro Fujita[1] · Jiwang Yan[1]

Received: 30 May 2019 / Accepted: 23 December 2019 / Published online: 18 January 2020

Abstract
It has been previously reported that electrical discharge machining (EDM) performance can be improved by tool electrode vibration. However, the mechanism of vibration-assisted EDM has not been clarified and the optimal vibration condition remains unknown due to the difficulty in direct process observation. In this study, direct observation of the EDM gap by using a high-speed video camera through a transparent workpiece electrode made of single-crystal 4H-SiC was attempted. It was found that tool vibration caused discharge dispersion and discharge frequency increase, and this tendency was more significant at higher amplitudes and higher frequencies. In addition, tool vibration-induced periodic discharge was observed, which prevented concentrated discharge and short-circuiting. Accordingly, the machining speed was improved and surface roughness was reduced. This study succeeded for the first time in observing the discharge behaviors in vibration-assisted EDM, thus revealed the effects of key parameters for process optimization.

Keywords Electrical discharge machining · Vibration-assisted EDM · Transparent workpiece electrode · High-speed video camera · Discharge distribution

1 Introduction

Electrical discharge machining (EDM) is a noncontact machining method that works on the thermal effect of electrical discharges [1]. EDM can be used for any electrically conductive materials regardless of their hardness [2–4]. In addition, EDM can precisely transfer the shape of the tool to the workpiece, which enables the fabrication of various surface shapes [2, 5–7]. Due to these advantages, EDM is widely used for fabricating high-added-value products like molds for press/injection molding [8, 9].

However, there is a serious problem in EDM that debris is hardly removed from the gap between the tool and workpiece. This causes short-circuiting and concentrated discharge which makes the machining process unstable. To solve this problem, some methods have been proposed to help eject debris by activating the working fluid flow. For example, in die-sinking EDM, tool vibration has been introduced.

It has been reported that vibration-assisted micro-EDM enhances machining performance, and the reason for this has been considered as ultrasonic vibration-induced cavitation effects. The machining speed and surface quality were improved because bubbles helped emit debris [10–12]. However, even without cavitation effects, vibration-assisted EDM still showed higher machining performance than conventional EDM [13–17]. From this meaning, there might be other factors governing the mechanisms of vibration-assisted EDM. One of the possible factors is oil flow caused by tool vibration. The oil flow diffuses and ejects debris, which would prevent short-circuiting or discharge concentration. This would result in uniform discharge distribution and higher discharge frequency.

However, these phenomena have not been observed or verified, and the mechanism of electrical discharging in vibration-assisted EDM remains still unclear because the direct observation of an EDM gap is extremely difficult. The distance between the tool and the workpiece is often less than 10 μm, which is too small to accommodate a camera. Moreover, the discharges emit bright

✉ Jiwang Yan
yan@mech.keio.ac.jp

[1] Department of Mechanical Engineering, Keio University, 3-14-1 Hiyoshi, Kohoku, Yokohama, Kanagawa 223-8522, Japan

Table 1 Properties of 4H-SiC

Surface plane	(0001)
Doping type	N-type
Electrical resistivity (Ω/cm)	0.015 ~ 0.028
Mohs hardness	~ 9.2
Thermal conductivity (W/cm·K)	3.7
Melting point (°C)	2730
Sublimation temperature (°C)	2830
Dielectric constant	9.76
Band gap (eV)	3.23

Table 2 Experimental conditions

	Group 1	Group 2
Voltage (V)	110	
Condenser capacitance (pF)	3300	
Feed rate (μm/s)	0.5	
Polarity	4H-SiC (+)	
	Cu (−)	
Dielectric fluid	EDM oil (CASTY-LUBE EDS)	
Amplitude (μm)	0.5, 1.0, 1.5	1.5
Frequency (Hz)	500	50, 100, 250, 500

lights and cause bubbles, which disturb the direct observation of the charges. Due to the difficulty in experimental observation, some previous studies aimed to investigate the gap phenomenon with numerical simulations [18–20]. In recent years, the EDM gap phenomena were directly observed by using a transparent electrode from the direction normal to the workpiece, and the discharge spots were successfully observed by Kunieda et al.

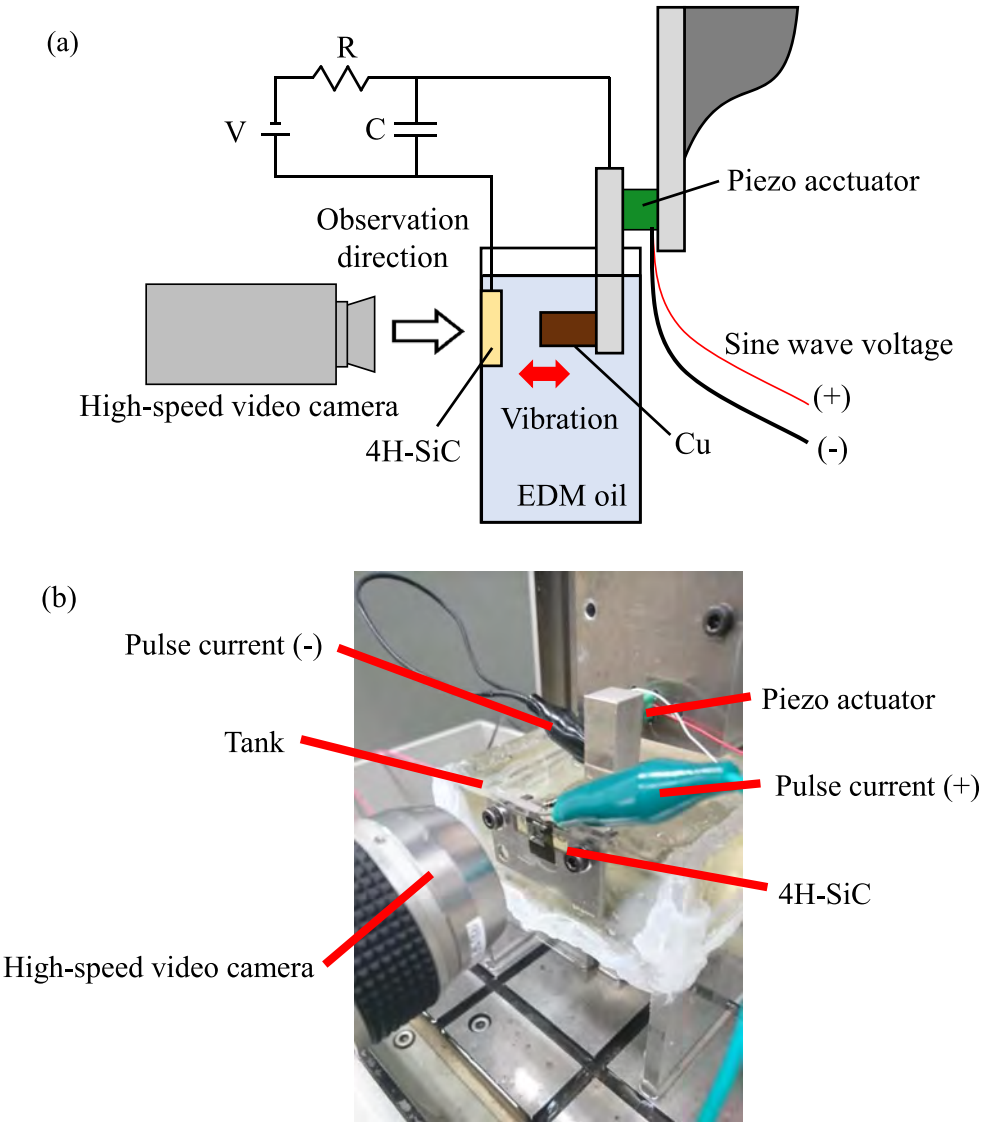

Fig. 1 (a) Schematic diagram and (b) photograph of the experimental setup

[21–24]. This observation method might provide the possibility of examining the gap phenomena in vibration-assisted EDM.

In this study, the direct observation of gap phenomena via a transparent workpiece electrode made of single-crystal 4H-SiC was applied to vibration-assisted EDM, and the locations of discharges were successfully observed. For these results, the discharge distribution and the discharge frequency were evaluated. In addition, other differences in the discharge phenomenon corresponding to various vibration conditions were analyzed and compared. The findings from this study will reveal the fundamental mechanism of vibration-assisted EDM and contribute to the optimization of EDM processes.

2 Experimental method

An experiment was performed using a high-precision micro-EDM machine (Panasonic MG-ED72) which has a resistor–capacitor (RC) pulse generator. The workpiece material was an n-type single-crystal 4H-SiC (4 mm × 4 mm × 350 μm) with a CMP finish. The properties of the 4H-SiC are shown in Table 1. This material has sufficiently low electrical resistivity so that it can be machined by EDM, and sufficiently high transparency to visible light, enabling direct observation of discharge phenomena [21]. A copper cylinder (1 mm in diameter) was used as the tool electrode. To generate vibration, the tool was equipped on a piezoelectric actuator, as shown in Fig. 1 (a). Die-sinking EDM was performed and the EDM gap phenomena were observed through the 4H-SiC electrode using a high-speed video camera (Keyence VM9000). The frame rate of the high-speed video camera was set to 1000 fps, and the resolution to 640 × 480 pixel.

The experimental conditions used in the experiment are shown in Table 2. Two groups of experiments were performed. First, the effect of vibration amplitude was investigated in comparison with non-vibration assisted EDM. In the second experiment, the effect of vibration frequency was investigated. The amplitude was set to 1.5 μm because this amplitude showed the best results in the preliminary experiments. In each group of experiments, the distribution of discharges, the number of discharges and resulting machining speed were investigated. In addition, to investigate the vibration effects on machined surface topography, the EDMed surface (machining depth 200 μm) was observed by a scanning electron microscope (SEM: FEI Inspect F50) and measured by a white light interferometer (Ametek Talysurf CC11000) and a non-contact laser-probe profilometer (Mitaka MP-3).

3 Results and discussion

3.1 Effect of vibration amplitude

An arbitrary video frame of EDM gap is shown in Fig. 2 (a). Discharge spots were successfully observed through the transparent workpiece electrode. The image

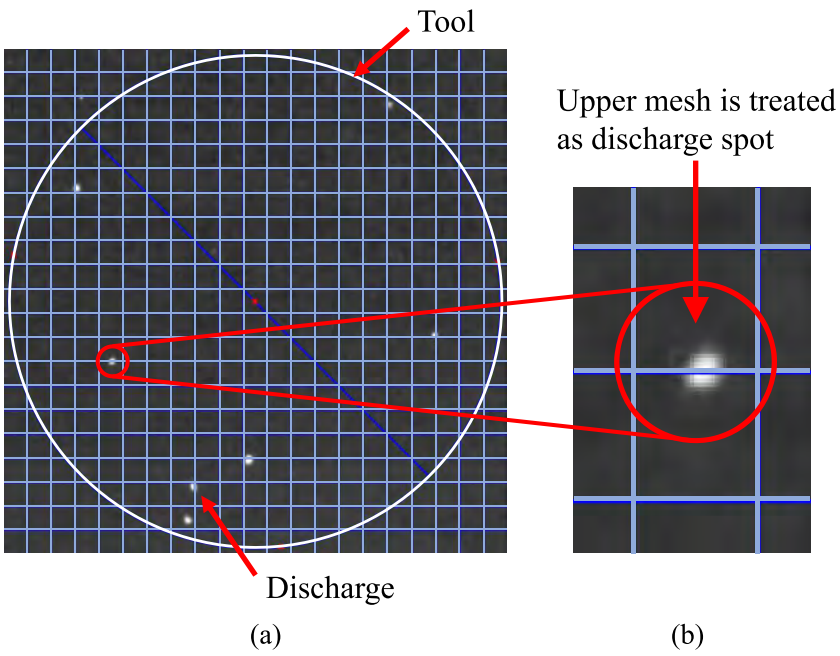

Fig.2 A high-speed video frame: (a) general view, (b) magnified view showing a discharge occurring near the boundary of two meshes

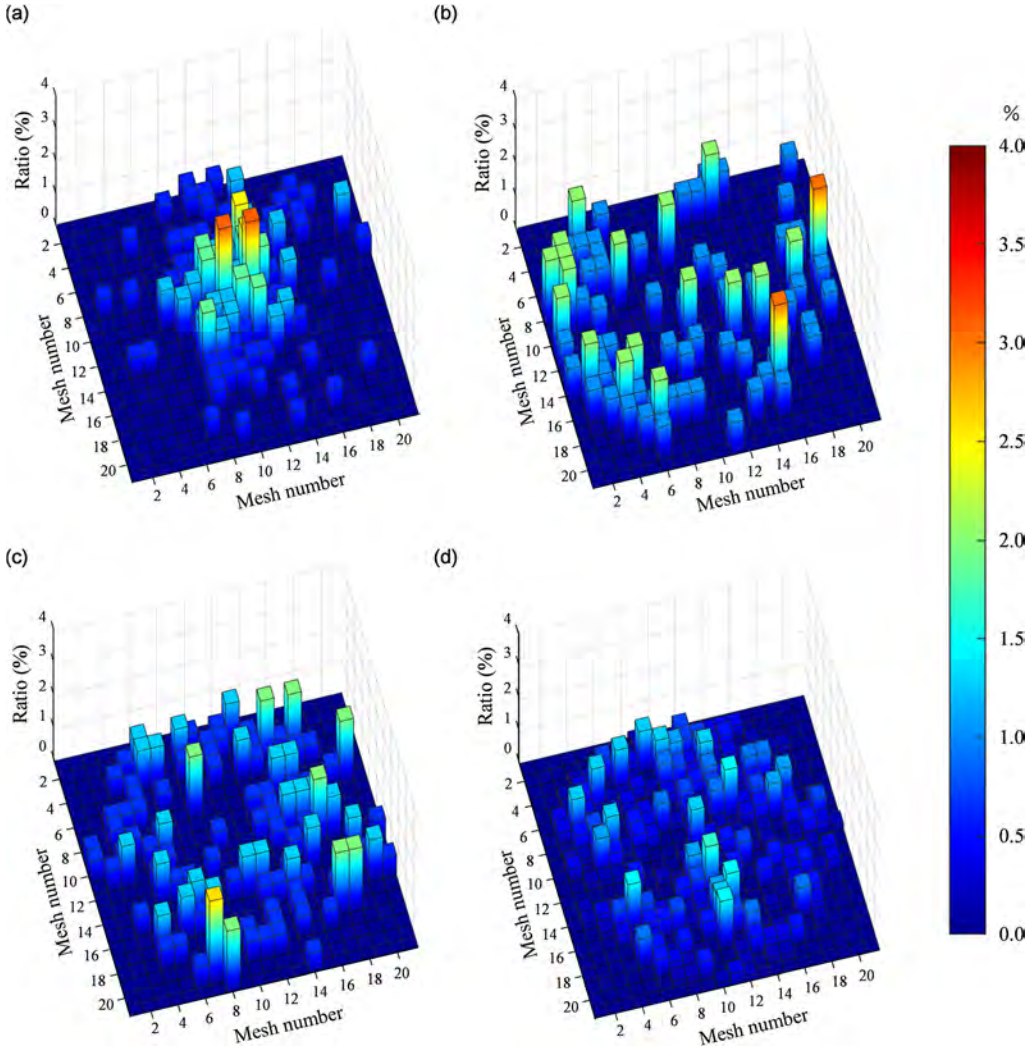

Fig. 3 Distributions of discharge ratios in EDM with different vibration amplitudes: (a) without vibration, (b) 0.5 μm, (c) 1.0 μm, and (d) 1.5 μm at a constant frequency of 500 Hz

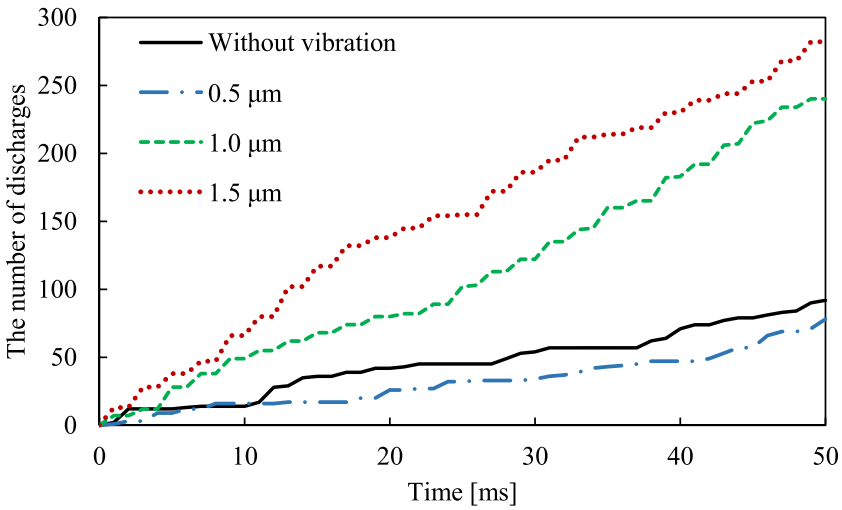

Fig. 4 The number of discharges at different amplitudes

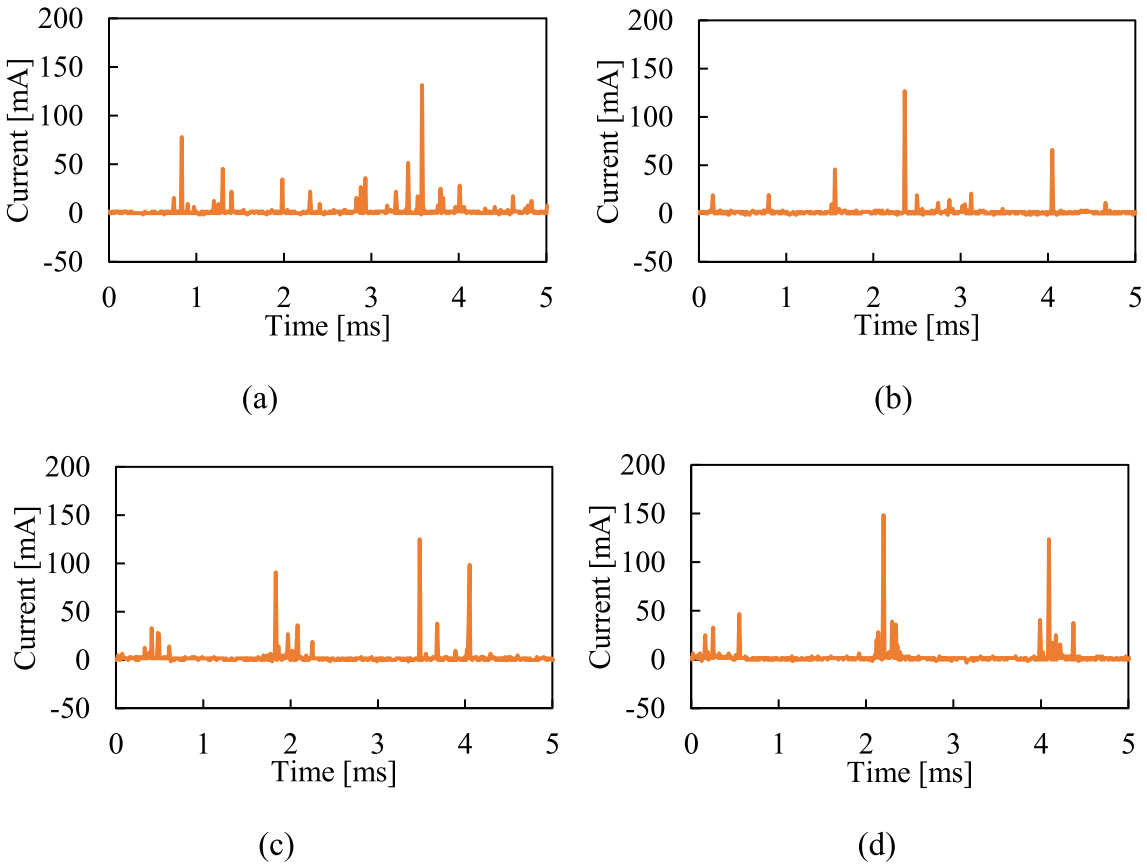

Fig. 5 Electric current waveforms observed at different vibration amplitudes: (a) without vibration, (b) 0.5 μm, (c) 1.0 μm, and (d) 1.5 μm at a frequency of 500 Hz

was divided by 21 × 21 meshes to investigate discharge distribution. The discharge occurrence in each mesh for a period of 50 ms was counted. When a discharge occurred near the boundary of two adjacent meshes, as shown in Fig. 2 (b), the discharge was counted to the mesh in which the discharge center was located.

Figure 3 shows the distributions of discharge ratios in EDM without vibration assistance and vibration-assisted EDM at different amplitudes (frequency 500 Hz) during a period of 50 ms. The distributions of vibration-assisted EDM (Fig. 3 (b)–(d)) were more uniform than that of EDM without tool vibration (Fig. 3 (a)). Figure 4 shows the change in the total number of discharges in all meshes for 50 ms. Vibration with amplitudes of 1.0, 1.5 μm induced more discharges than that without vibration; while vibration with an amplitude of 0.5 μm resulted in fewer discharges than that without vibration. In addition, the number of discharges at 1.0, 1.5 μm increased step by step at every 2 ms. This tendency was also confirmed from the electrical current waveforms at different amplitudes as shown in Fig. 5. In Fig. 5, sharp electrical current peaks appeared approximately at every 2 ms for vibration amplitudes of 1.0 and 1.5 μm. Among the peaks, almost no discharge occurred. This phenomenon might have occurred

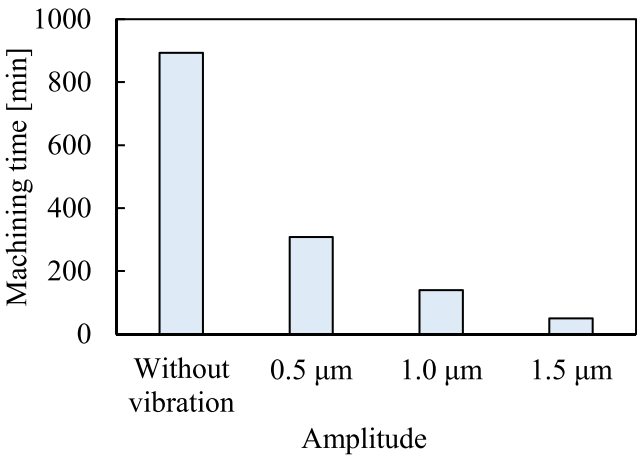

Fig. 6 Time for machining 200 μm deep at different vibration amplitudes

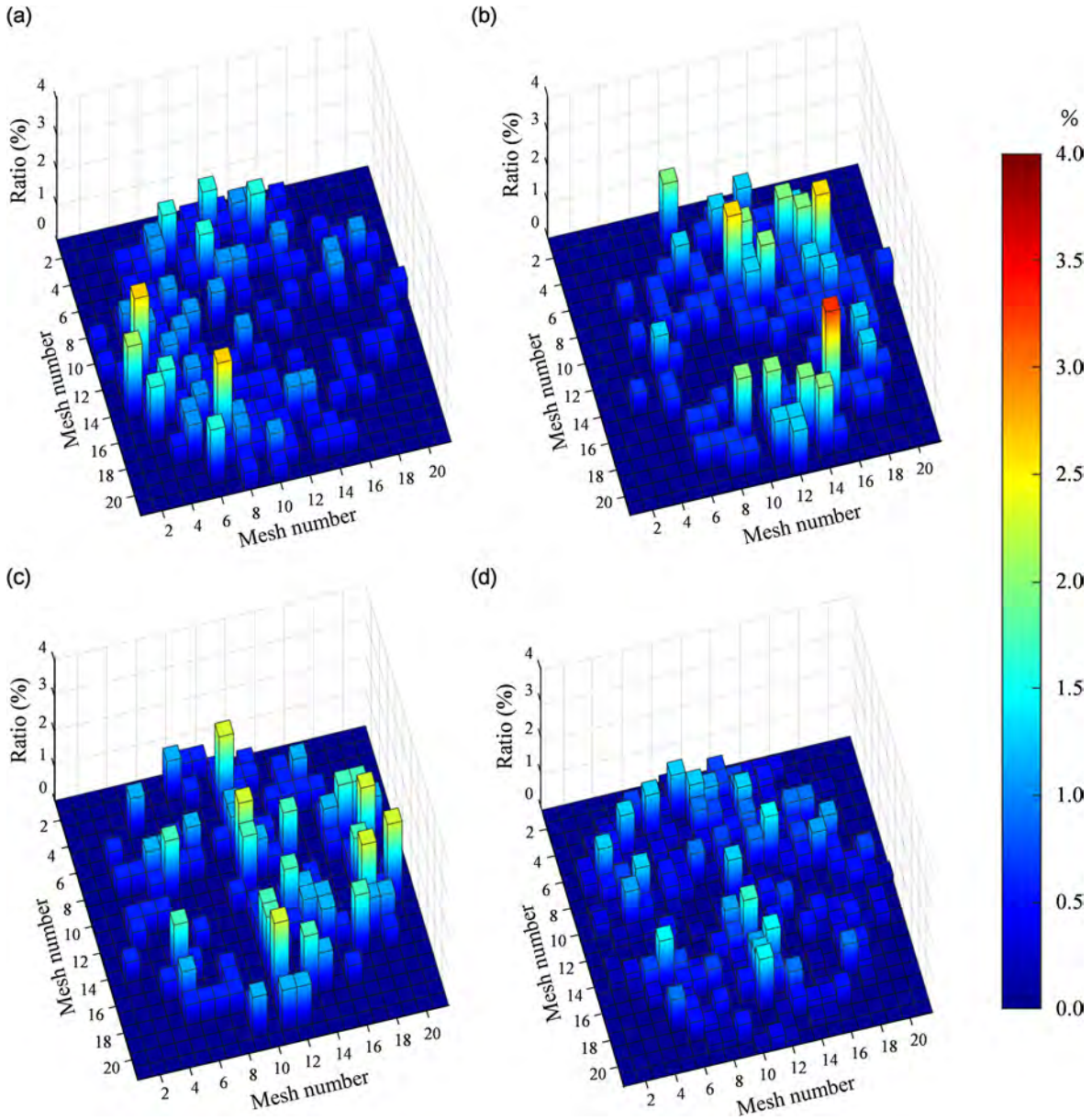

Fig. 7 Distribution of discharge ratios at different vibration frequencies (a) 50 Hz, (b) 100 Hz, (c) 250 Hz, and (d) 500 Hz at a 1.5 μm amplitude

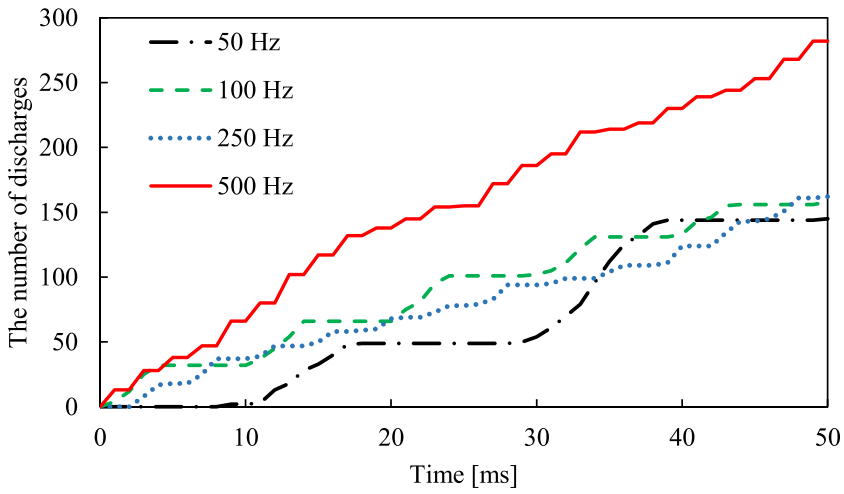

Fig. 8 The number of discharges at different frequencies

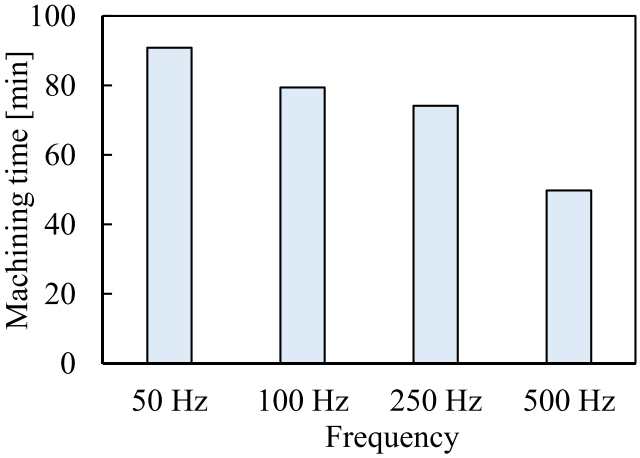

Fig. 9 Machining time for a depth of 200 μm at different vibration frequencies

because the gap between the tool and the workpiece increased periodically over the threshold distance for discharge occurrence in vibration-assisted EDM. In the case of 0.5 μm amplitude, however, no periodicity could be identified in discharge occurrence. Figure 6 shows the time taken to machine a 200 μm-deep hole at different amplitudes with a frequency of 500 Hz. The machining time was greatly reduced by vibration-assisted EDM and at large amplitudes.

3.2 Effect of vibration frequency

Figure 7 shows the distribution of discharge ratios in vibration-assisted EDM at different frequencies with a fixed amplitude of 1.5 μm. The discharge distribution was

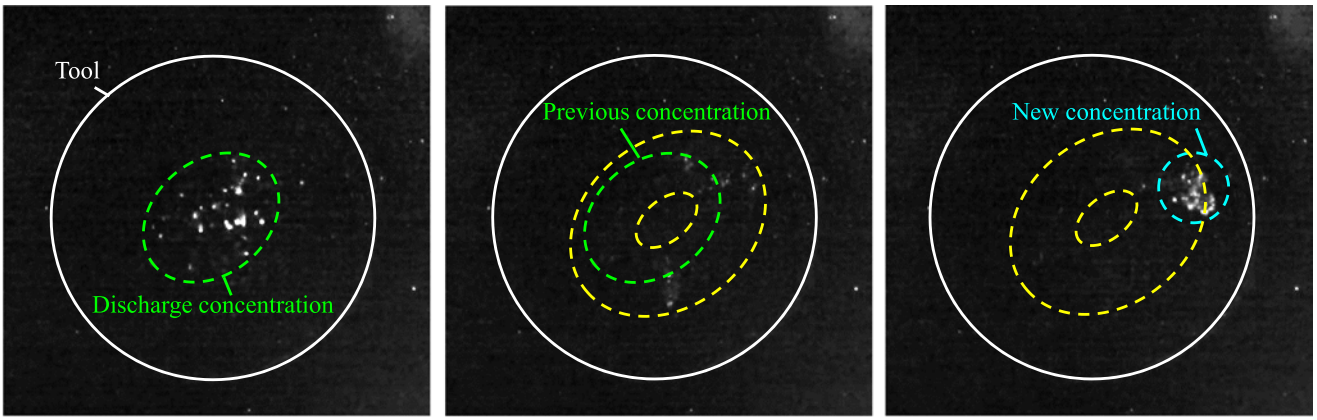

(a) Concentration (b) Spreading [25 ms after (a)] (c) New concentration [28 ms after (a)]

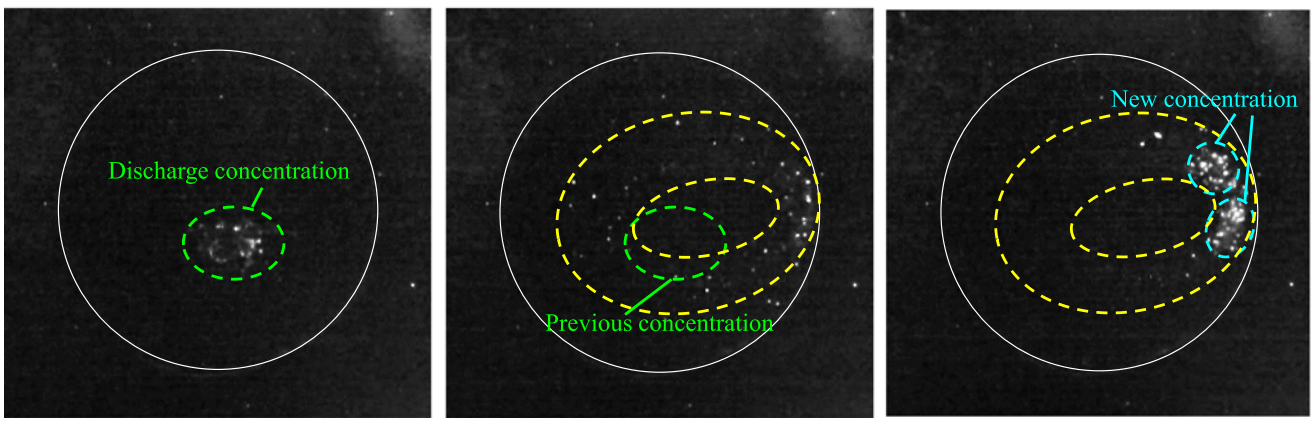

(d) Concentration (e) Spreading [268 ms after (d)] (f) New concentration [398 ms after (d)]

Fig. 10 High-speed video frames taken before short-circuiting: (a)–(c) EDM without tool vibration, (d)–(f) vibration-assisted EDM at 1.5 μm and 500 Hz

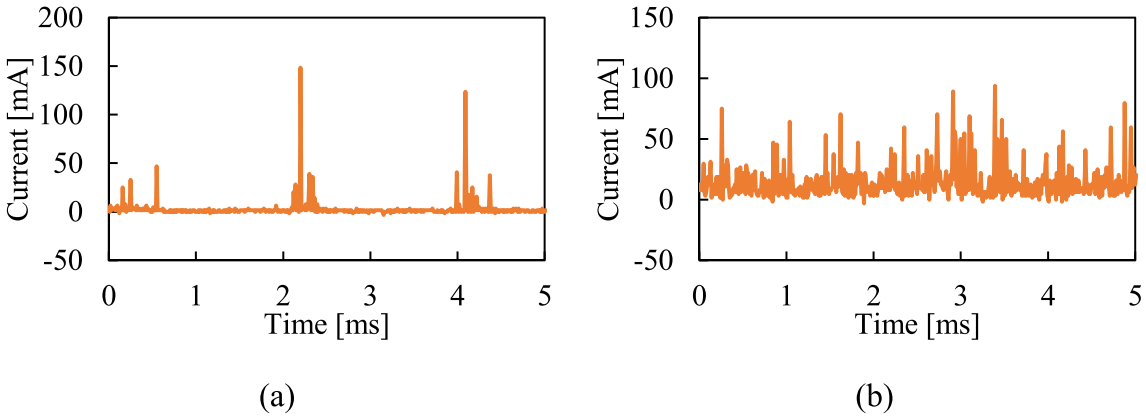

Fig. 11 Electrical current waveform measured in vibration-assisted EDM at 1.5 μm and 500 Hz: (a) stable machining, (b) concentrated discharge before short-circuiting

relatively more uniform at 500 Hz than other frequencies. Figure 8 shows the total number of discharges during a period of 50 ms. In all conditions, the number of discharges increased step by step at the same cycle time as tool vibration (50 Hz: 20 ms, 100 Hz: 10 ms, 250 Hz: 4 ms, 500 Hz: 2 ms). This suggests that tool vibration with an amplitude of 1.5 μm has caused a periodical discharge phenomenon. The amount of discharges is largest at the highest

Fig. 12 Discharge craters in EDM without tool vibration

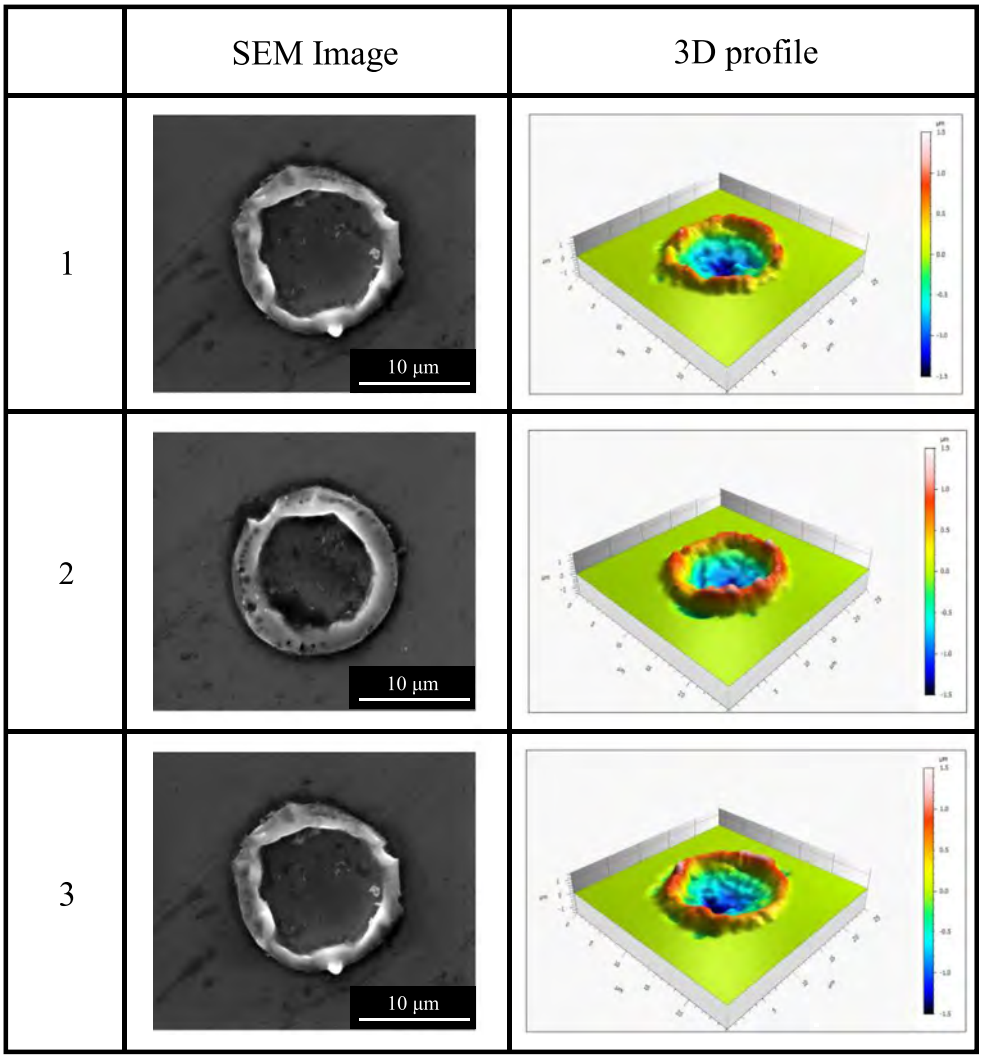

frequency 500 Hz, although there was no clear difference among 50, 100, and 250 Hz. Figure 9 shows the machining time of a 200 μm-deep hole at different frequencies with 1.5 μm amplitude. The machining time is reduced particularly at 500 Hz, which is similar to the tendency of discharge number in Fig. 8.

3.3 Discharge phenomena before short-circuiting

Short-circuiting is the main drawback in EDM, which severely lowers the machining efficiency and stability. Thus, the investigation of discharge phenomena before short-circuiting is essential for preventing the occurrence of short-circuiting. In this study, a peculiar discharge concentration phenomenon was observed before the occurrence of short-circuiting. Figure 10 shows typical high-speed video frames. First, once discharge concentration occurred (Fig. 10 (a)), the area of the concentrated discharge spread in a distorted ring shape (Fig. 10 (b)). After this, a new discharge concentration region occurred in the previous concentration area (Fig. 10 (c)). The new discharge concentration region also spread in a ring shape and finally resulted in short-circuiting. Therefore, the cyclic discharge concentration phenomenon might be a transition stage to short-circuiting. Similar phenomenon was also observed in vibration-assisted EDM (Fig. 10 (d)–(f)), although the discharge concentration was less frequent than that in EDM without tool vibration. In addition, unlike in EDM without tool vibration, the no-discharge period in vibration-assisted EDM disappeared before short-circuiting, as shown in Fig. 11, indicating an active discharge mode even before short-circuiting. Furthermore, during continuous observation, it was found that the period of discharge concentration before short-circuiting was 10~30 ms in EDM without tool vibration, and 200~1000 ms for EDM with tool vibration. This may suggest that tool vibration can delay and prevent short-circuiting as compared with EDM without tool vibration.

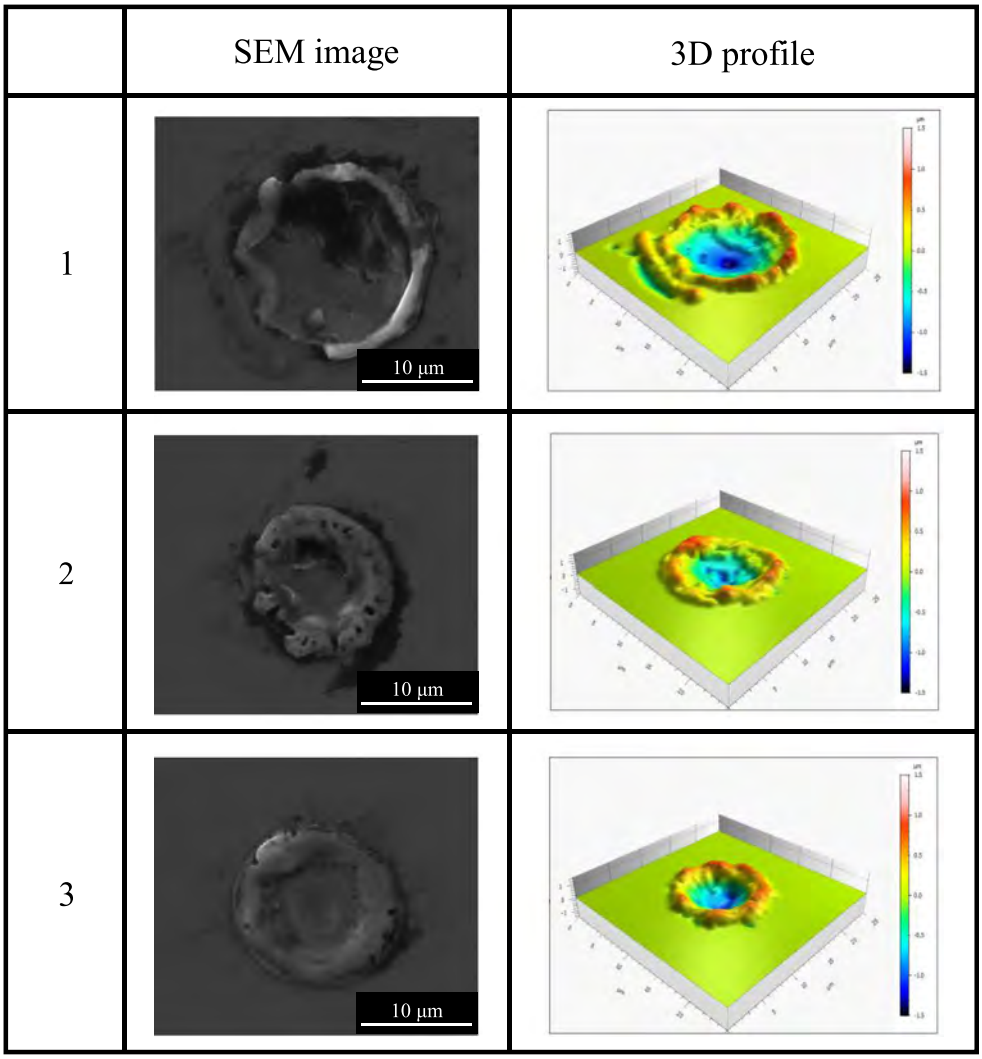

Fig. 13 Discharge craters in vibration-assisted EDM (1.5 μm–500 Hz)

3.4 Effect of tool vibration on surface quality

Vibration effects on surface topography were investigated by surface observation after machining. First, typical single discharge craters in EDM without tool vibration and vibration-assisted EDM were observed as Figs. 12 and 13, respectively. In EDM without tool vibration, the sizes of craters are almost the same (Fig. 12); whereas the sizes of craters differ obviously in vibration-assisted EDM (Fig. 13). This indicates that tool vibration causes the change of discharge gap width, and in turn, alters the size of discharge craters.

Figure 14 shows the SEM images of the surface after EDM without tool vibration and vibration-assisted EDM at 1.5 μm and 500 Hz. The surfaces were observed after ultrasonic cleaning in ethanol for 10 min. There were many re-solidified debris on the surface of EDM without tool vibration (Fig. 14 (a), (b)). In contrast, there were few re-solidified debris on the surface of vibration-assisted EDM (Fig. 14 (c), (d)). Presumably, oil flow caused by tool vibration has minimized the debris from the surface. This is similar to the oil flow effects generated by tool rotation in EDM of 4H-SiC, where few re-solidified debris was found on the machined surface at a voltage of 110 V [25].

Figure 15 shows a comparison of surface roughness after EDM without tool vibration and vibration-assisted EDM. Figure 16 shows typical cross-sectional profiles of the measured surfaces. The surface roughness was calculated as the average value of 5 different measurements. The surface roughness and its standard deviation both became smaller after introducing tool vibration with an amplitude of 1.0 and 1.5 μm.

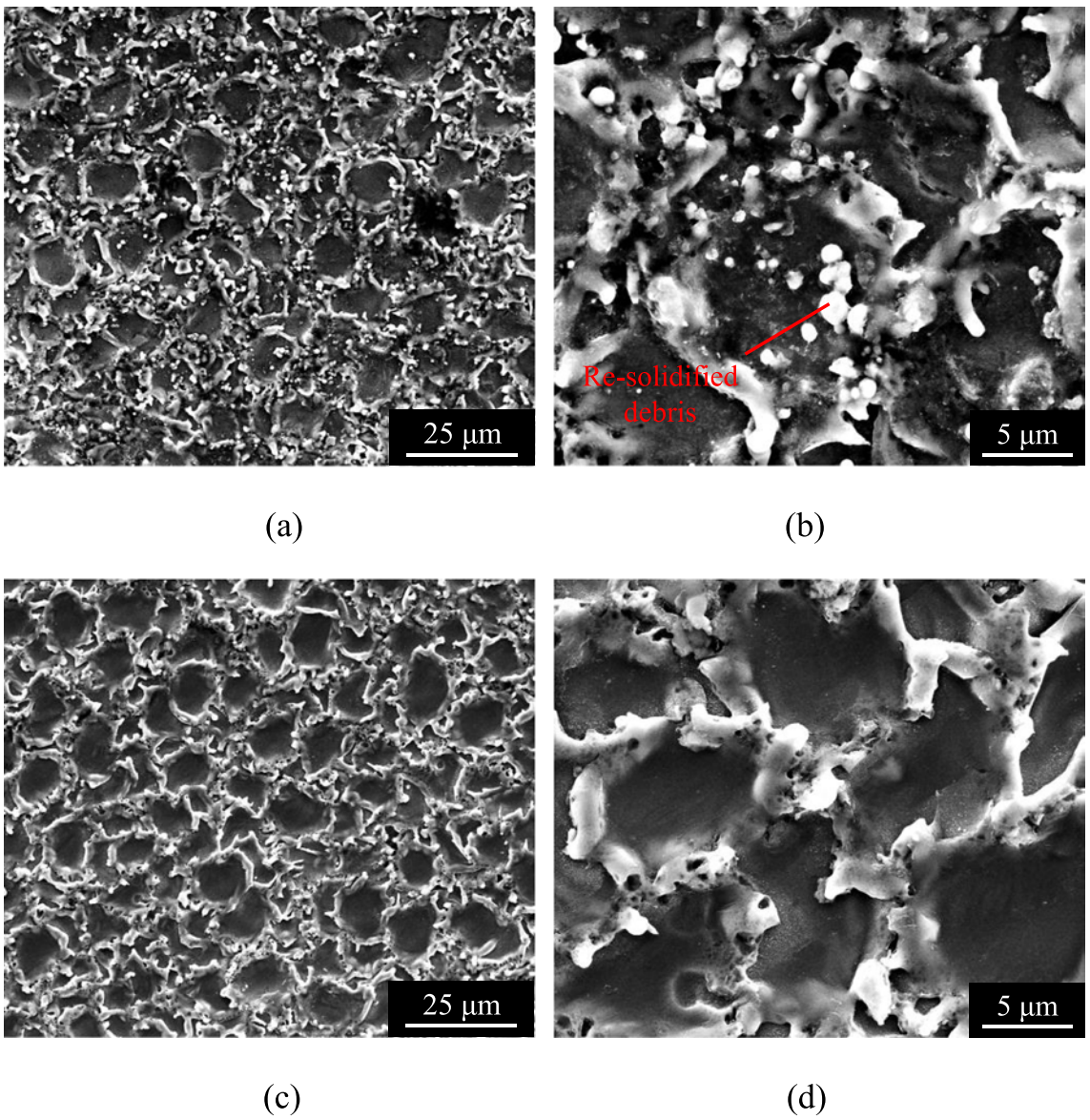

Fig. 14 SEM images of EDM-ed surfaces: (a) without tool vibration, (c) vibration-assisted EDM at 1.5 μm and 500 Hz. (b) and (d) are magnified view of (a)

This would be due to the uniform distribution of discharges as well as suppression of debris re-solidification on the surface in vibration-assisted EDM.

3.5 Mechanism of vibration-assisted EDM

The aforementioned results have demonstrated that EDM performance can be improved by introducing tool vibration. The effect of tool vibration might originate from multiple aspects. Once a discharge occurs, a bubble is generated, and further discharges easily occur at the bubble boundaries where debris is concentrated [22]. The bubble generation is also affected by the viscosity of a dielectric fluid. A dielectric fluid of low viscosity is preferable in vibration-assisted EDM. The concentrated discharges on the boundary of bubbles cause subsequently concentrated discharges and further formation of debris, as shown in Fig. 17 (a)–(c). This may be a typical mechanism for short-circuiting in EDM without tool vibration. In vibration-assisted EDM, however, the occurrence of short-circuiting is suppressed because there is a no-discharge period in every cycle of tool vibration (see Fig. 5). As discharge concentration tends to occur at the boundary of bubbles, as shown in Fig. 17 (d), it would be stopped due to the no-discharge period, as shown in Fig. 17 (e). During the no-discharge period, tool vibration spreads the debris and bubbles, which prevents discharge concentration at the boundary of bubbles. This effect can be seen from the uniform distribution of discharges (see Fig. 3). As a result, vibration-assisted EDM prevents short-circuiting and demonstrates higher machining speed, as shown in Fig. 17 (d)–(f). In addition, the uniform distribution of discharge in vibration-assisted EDM can prevent the shape deviation of a workpiece and uneven tool wear. If there is unevenness on the workpiece surface or tool surface, discharge concentration will occur intensively because the working gap would be highly location dependent.

Next, the effect of vibration amplitude is considered. An amplitude of 1.5 μm showed the highest efficiency (see Fig. 6). This would be because tool vibration with a larger amplitude emits more fluid and debris from a discharge gap. Therefore, a larger amplitude is favorable for vibration-assisted EDM. If the vibration amplitude is too small, for example 0.5 μm, the unification of discharge distribution and diffusion of debris will be insignificant and not enough to prevent short-circuiting. However, even in this case, catastrophic short-circuiting, which stops machining and requires machine restart, is prevented and total machining time is decreased as compared with EDM without tool vibration. Theoretically, the optimum amplitude of vibration is dependent on the discharge gap. If the discharge voltage is high and the discharge gap is big, a large amplitude of vibration is preferable, and vice versa. If the amplitude is too large, however, it would decrease the machining speed because the no-discharge period in every cycle of tool vibration becomes longer.

The effect of vibration frequencies may be due to the difference in discharge periods. Tool vibration at a sufficiently large amplitude (~ 1.5 μm) causes no-discharge period which suppresses discharge concentration and improves machining speed. In cases of frequencies lower than 500 Hz, however, the discharge may continue too long. As a result, more short-circuiting occurs, which hinders the EDM process. Thus, the optimization of vibration amplitude and frequency in vibration-assisted EDM is important to improve the machining efficiency, stability, and surface quality.

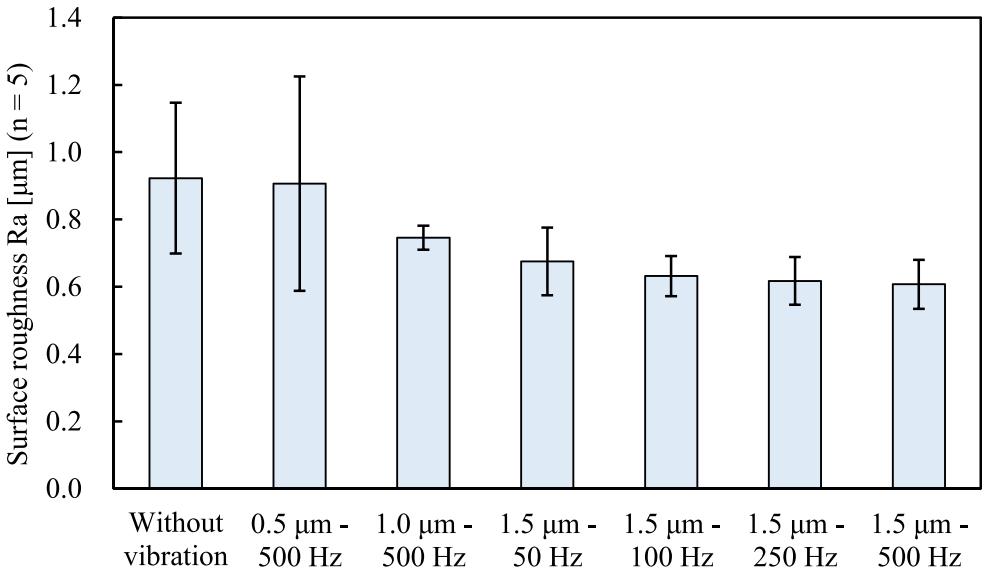

Fig. 15 Effect of tool vibration on surface roughness

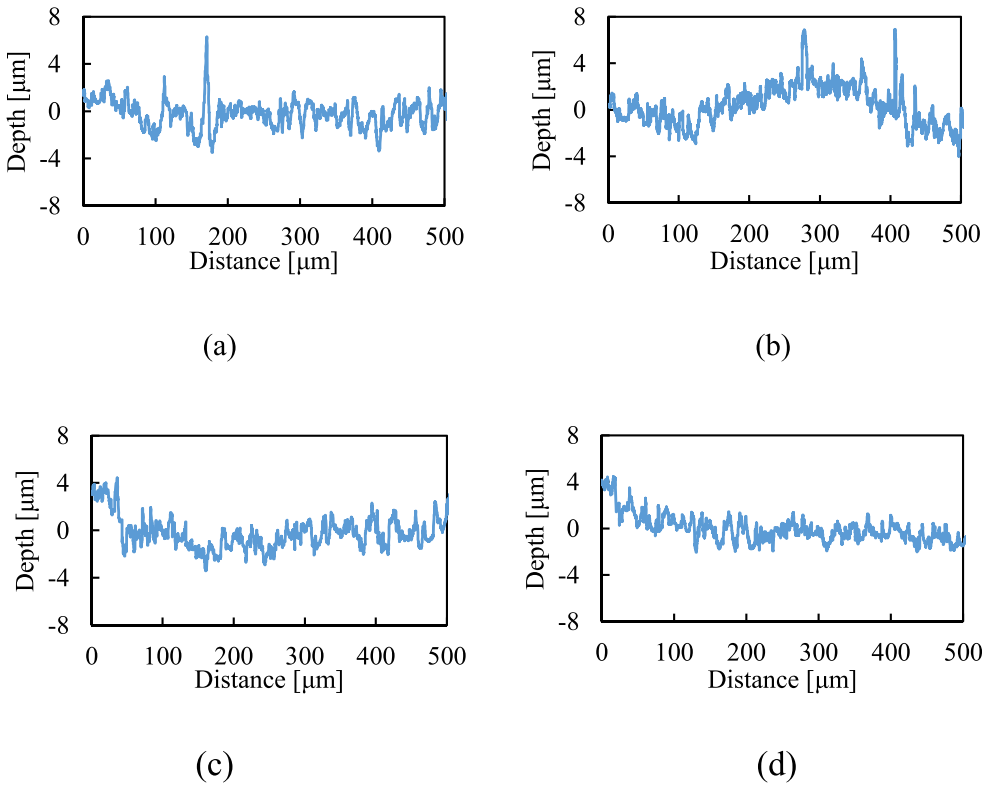

Fig. 16 Cross-sectional profiles of machined surface; (a) Without vibration, (b) 0.5 μm–500 Hz, (c) 1.0 μm–500 Hz, (d) 1.5 μm–500 Hz

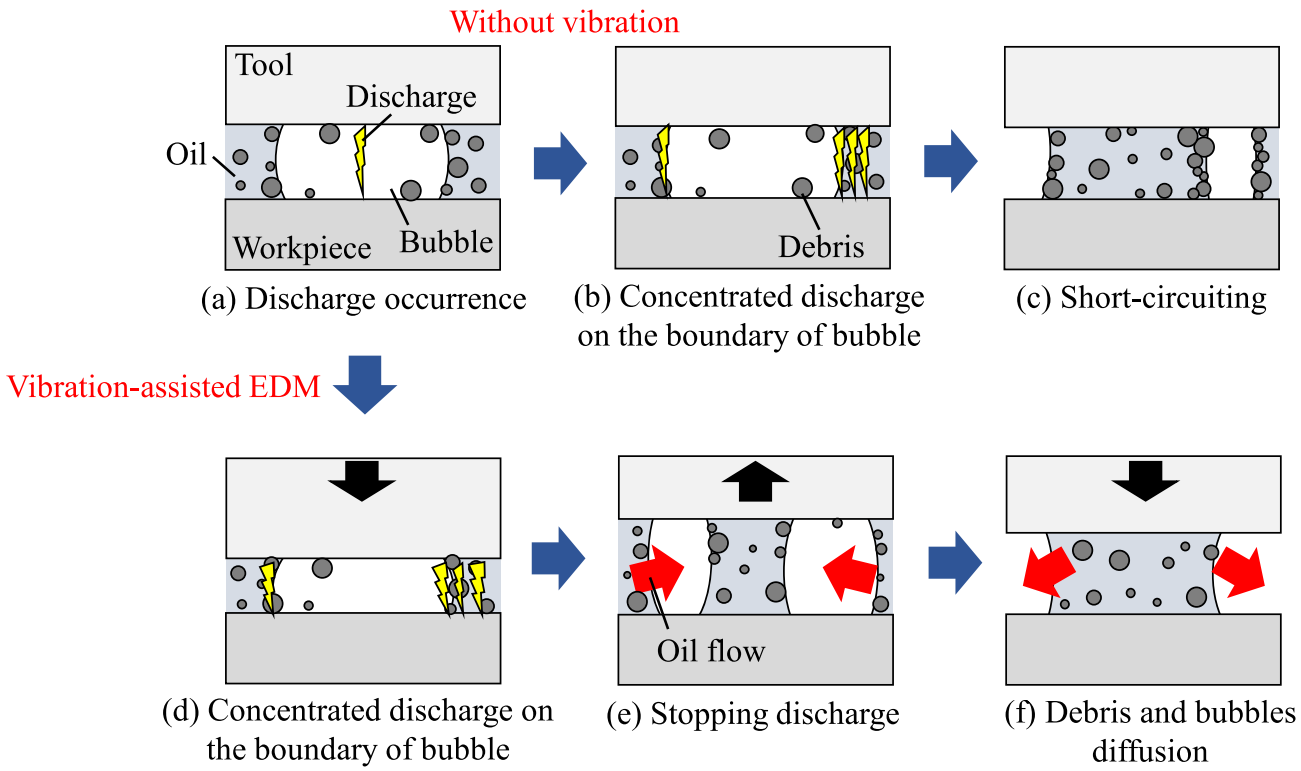

Fig. 17 Schematic diagram of tool vibration effect in EDM

4 Conclusions

The changes in electrical discharge phenomena caused by tool vibration were directly observed by a high-speed video camera through a transparent workpiece electrode of single-crystal 4H-SiC. The following conclusions were obtained:

(1) The distribution of discharges was more uniform in vibration-assisted EDM as compared with EDM without tool vibration. Tool vibration also increased the total number and frequency of discharges.
(2) The peculiar concentration behavior of discharges was observed. The concentrated discharge area spreads in a distorted ring shape followed by new discharge concentrations in the ring area.
(3) A sufficiently large vibration amplitude (~ 1.5 μm) results in periodic discharge phenomena, enabling uniform discharge distributions, and high machining speeds.
(4) A high vibration frequency (~ 500 Hz) causes a higher number of discharges and machining speed than lower frequencies.
(5) Vibration-assisted EDM improves surface roughness and reduces debris adhesion on the machined surface.

This study clarified the gap phenomena and the effect of tool vibration on EDM mechanism, which is important for optimizing vibration conditions to improve the machining efficiency, stability, and surface quality. Future tasks include the investigation of the relationship between tool vibration and electronic frequency of discharge voltage and their effects on the machining characteristics and the establishment of a theoretical model for the vibration-assisted EDM process.

References

1. Hinduja S, Kunieda M (2013) Modelling of ECM and EDM processes. CIRP Ann 62:775–797. https://doi.org/10.1016/j.cirp.2013.05.011
2. Takahata K, Shibaike N, Guckel H (2000) High-aspect-ratio WC-Co microstructure produced by the combination of LIGA and micro-EDM. Microsyst Technol 6:175–178. https://doi.org/10.1007/s005420000052
3. Peng Z, Wang Z, Dong Y, Chen H (2010) Development of a reversible machining method for fabrication of microstructures by using micro-EDM. J Mater Process Technol 210:129–136. https://doi.org/10.1016/j.jmatprotec.2009.08.002
4. Yan J, Watanabe K, Aoyama T (2014) Micro-electrical discharge machining of polycrystalline diamond using rotary cupronickel electrode. CIRP Ann Manuf Technol 63:209–212. https://doi.org/10.1016/j.cirp.2014.03.058
5. Tong H, Li Y, Wang Y (2008) Experimental research on vibration assisted EDM of micro-structures with non-circular cross-section. J Mater Process Technol 208:289–298. https://doi.org/10.1016/j.jmatprotec.2007.12.126
6. Yi SM, Park MS, Lee YS, Chu CN (2008) Fabrication of a stainless steel shadow mask using batch mode micro-EDM. Microsyst Technol 14:411–417. https://doi.org/10.1007/s00542-007-0468-0
7. Lei J, Wu X, Wang Z et al (2019) Electrical discharge machining of micro grooves using laminated disc electrodes made of cu and Sn foils. J Mater Process Tech 271:455–462. https://doi.org/10.1016/j.jmatprotec.2019.04.024
8. Zhou T, Zhou C, Liang Z, Wang X (2018) Machining mechanism in tilt electrical discharge milling for lens mold. Int J Adv Manuf Technol 95:2747–2755. https://doi.org/10.1007/s00170-017-1408-5
9. Yu Z, Li D, Yang J, Zeng Z, Yang X, Li J (2019) Fabrication of micro punching mold for micro complex shape part by micro EDM. Int J Adv Manuf Technol 100:743–749. https://doi.org/10.1007/s00170-018-2731-1
10. Iwai M, Ninomiya S, Suzuki K (2013) Improvement of EDM properties of PCD with electrode vibrated by ultrasonic transducer. Procedia CIRP 6:146–150. https://doi.org/10.1016/j.procir.2013.03.070
11. Liew PJ, Shimada K, Mizutani M et al (2013) Fabrication of microstructures on RB-SiC by ultrasonic cavitation assisted micro-electrical discharge machining. Int J Autom Technol 7:621–629
12. Liew PJ, Yan J, Kuriyagawa T (2014) Fabrication of deep micro-holes in reaction-bonded SiC by ultrasonic cavitation assisted micro-EDM. Int J Mach Tools Manuf 76:13–20. https://doi.org/10.1016/j.ijmachtools.2013.09.010
13. Endo T, Tsujimoto T, Mitsui K (2008) Study of vibration-assisted micro-EDM-the effect of vibration on machining time and stability of discharge. Precis Eng 32:269–277. https://doi.org/10.1016/j.precisioneng.2007.09.003
14. Jiang Y, Zhao W, Xi X et al (2012) Vibration assisted EDM of small-hole using voice coil motor. Procedia CIRP 1:645–650. https://doi.org/10.1016/j.procir.2012.04.114
15. Tsai MY, Fang CS, Yen MH (2018) Vibration-assisted electrical discharge machining of grooves in a titanium alloy (Ti-6A-4V). Int J Adv Manuf Technol 97:297–304. https://doi.org/10.1007/s00170-018-1904-2
16. Jahan MP, Wong YS, Rahman M (2012) Evaluation of the effectiveness of low frequency workpiece vibration in deep-hole micro-EDM drilling of tungsten carbide. J Manuf Process 14:343–359. https://doi.org/10.1016/j.jmapro.2012.07.001
17. Prihandana GS, Mahardika M, Hamdi M, Mitsui K (2011) Effect of low-frequency vibration on workpiece in EDM processes. J Mech Sci Technol 25:1231–1234. https://doi.org/10.1007/s12206-011-0307-1
18. Xie B, Zhang Y, Zhang J et al (2015) Flow field simulation and experimental investigation of ultrasonic vibration assisted EDM holes Array. Int J Control Autom 8:419–424. https://doi.org/10.14257/ijca.2015.8.12.38
19. Liu Y, Chang H, Zhang W et al (2018) A simulation study of debris removal process in ultrasonic vibration assisted electrical discharge machining (EDM) of deep holes. Micromachines 9:378. https://doi.org/10.3390/mi9080378
20. Kumar S, Grover S, Walia RS (2018) Analyzing and modeling the performance index of ultrasonic vibration assisted EDM using graph theory and matrix approach. Int J Interact Des Manuf 12:225–242. https://doi.org/10.1007/s12008-016-0355-y
21. Kitamura T, Kunieda M (2014) Clarification of EDM gap phenomena using transparent electrodes. CIRP Ann - Manuf Technol 63:213–216. https://doi.org/10.1016/j.cirp.2014.03.059

22. Kitamura T, Kunieda M, Abe K (2015) Observation of relationship between bubbles and discharge locations in EDM using transparent electrodes. Precis Eng 40:26–32. https://doi.org/10.1016/j.precisioneng.2014.09.009
23. Mori A, Kunieda M, Abe K (2016) Clarification of gap phenomena in wire EDM using transparent electrodes. Procedia CIRP 42:601–605. https://doi.org/10.1016/j.procir.2016.02.219
24. Kunieda M, Kitamura T (2018) Observation of difference of EDM gap phenomena in water and oil using transparent electrode. Procedia CIRP 68:342–346. https://doi.org/10.1016/j.procir.2017.12.065
25. Yan J, Tan TH (2015) Sintered diamond as a hybrid EDM and grinding tool for the micromachining of single-crystal SiC. CIRP Ann Manuf Technol 64:221–224. https://doi.org/10.1016/j.cirp.2015.04.069